論文 / 著書情報
Article / Book Information

Title	Seismic Performance of damped-outrigger system incorporating buckling-restrained braces
Authors	P.C.Lin, T.Takeuchi
Pub. date	2020, 9
Citation	2020 17WCEE Proceedings

17th World Conference on Earthquake Engineering, 17WCEE
Sendai, Japan - September 13th to 18th 2020

SEISMIC PERFORMANCE OF DAMPED-OUTRIGGER SYSTEM INCORPORATING BUCKLING-RESTRAINED BRACES

P.C. Lin[(1)], T. Takeuchi [(2)]

[(1)] *Assistant professor, Department Civil Engineering, National Cheng Kung University, r97521211@ntu.edu.tw*
[(2)] *Professor, Department of Architecture and Building Engineering, Tokyo Institute of Technology, takeuchi.t.ab@m.titech.ac.jp*

Abstract

The outrigger system is an effective solution in mitigating seismic responses of core-tube type tall buildings by mobilizing the axial stiffness of the perimeter columns. The concept of damped-outrigger which introduces dampers in the outrigger system to dissipate seismic energy has been proposed. This study investigates the seismic behavior of a damped-outrigger system incorporating buckling-restrained brace (BRB) as energy dissipation device (BRB-outrigger). The BRB is arranged between the outrigger truss end and perimeter column. The BRB dissipates seismic energy through the relative displacement between outrigger truss and perimeter column. The wide axial force capacity range and feasible stiffness of BRB allow the BRB-outrigger system to be an alternative to conventional damped-outrigger system in resisting seismic loads. The outrigger effect combined with the stable energy dissipation mechanism of the BRB effectively reduce the seismic response of the building. This study proposes the methods to evaluate the inelastic seismic response of structures with multiple BRB-outriggers based on a spectral analysis (SA) procedure. For the structure with BRB-outriggers, the optimal outrigger elevations, and the relationships between the axial stiffness of the BRB, the axial stiffness of the perimeter column, and the flexural rigidity of the core structure in order to minimize the seismic response are the primary research objectives of this study. The maximum roof drift, the maximum inter-story drift, the maximum overturning moment at core structure base, and the maximum perimeter column axial force are used as indicators to indicate the seismic performance. Analytical models with building heights of 64 m, 128 m, 256 m, and 384 m are used to perform the SA. The analysis results are confirmed by performing the nonlinear response history analysis. Based on the analysis results, a step-by-step design recommendation and the design charts are provided for engineers to design the BRB-outrigger system in the preliminary design stage without the need of time-consuming iteration tasks. This research also introduces three types of BRB-outrigger configurations in order to meet different architecture requirements and economical solutions.

Keywords: Outrigger, Buckling-restrained Brace, Parametric Study, Optimal Design, Spectral Analysis

1. Introduction

The outrigger system has been an effective and economical solution for slender core-tube-type tall buildings in mitigating seismic responses and has been widely used as a seismic resistance system in tall buildings worldwide. In order to avoid the excessive force demands in the conventional outrigger members and to implement energy dissipation mechanisms into the outrigger system, the concept of the damped-outrigger was proposed by inserting dampers between the outrigger truss end and the perimeter column [1]. The dampers dissipate energy through the relative movement between the outrigger truss end and the perimeter column. The optimal outrigger elevations in order to minimize seismic response using viscous dampers [2, 3] and buckling-restrained brace (BRB) [4, 5] have been studied. This study reported the seismic behavior of a multiple-outrigger system incorporating BRB as energy dissipation device (BRB-outrigger). Fig. 1 shows the deformed structure with two BRB-outriggers (dual BRB-outrigger system). The core structure provides the majority of the lateral force resistance capacity. Each of the BRBs is arranged vertically between the outrigger truss ends and perimeter columns, so that the axial deformation demand of the BRB could be maximized. As shown in Fig. 1, when the structure deforms laterally to the right under lateral loading, the BRBs and perimeter columns on the right-hand side are in compression, and in tension on the left-hand side. The outrigger truss, BRBs, and perimeter columns act in series to provide resisting moments on the core structure at each outrigger elevation, so that the lateral deformation and base overturning moment of the core structure can be reduced. Once the BRBs yield, they start dissipating energy. The maximum force demands for the outrigger truss members and perimeter columns are limited by the maximum axial force capacity of the BRBs. The aims of this study are to propose a method to evaluate the seismic response of the multiple BRB-outrigger system with various outrigger elevations, investigate the optimal outrigger elevations in order to minimize the seismic response, and study the relationships between the flexural rigidity of the core structure and the axial stiffness of the perimeter columns and the BRBs in the dual BRB-outrigger system. The dynamic characteristics are studied and the seismic response is evaluated using the spectral analysis (SA), incorporating the concept of equivalent damping ratio to include the inelastic responses of the BRBs. The SA results are then validated by performing a nonlinear response history analysis (NLRHA). The maximum roof drift ratio (θ_{max}), inter-story drift (γ_{max}), overturning moment at the core structure base ($M_{c,max}$), and the additional axial force demand for the perimeter column ($C_{1,max}$) are adopted as indicators for judging the optimal outrigger elevations.

2. Analytical models

2.1 Simplified structure

Fig. 2 shows the simplified structure of height h with BRB-outriggers on n-levels, where l_t is the outrigger truss span. The lateral flexural rigidity and mass of the building are assumed to be concentrated at the core structure. The core structure is modeled by a cantilever column, which is assumed to deform in linear elasticity. The bases of the perimeter columns are free to rotate. The two ends of each BRB are pin-connected to the perimeter column and outrigger truss ends. The ends of the outrigger truss close to the core structure have full moment transfer capacity. For the j^{th} level of the BRB-outrigger, k_{tj} and k_{dj} are the flexural stiffness of outrigger truss and the BRB axial stiffness, respectively. The elevation of outrigger at the j^{th} level (h_j) is defined as follows:

$$h_j = \prod_{i=j}^{n} \alpha_i h \tag{1}$$

Where α_i is the elevation ratio of the ith layer to the $(i+1)^{th}$ layer of BRB-outrigger, and α_n is ratio of the n^{th} layer BRB-outrigger elevation to the building height. The analysis model used in this study is known as discrete mass (DM) model. The DM model was constructed by following the simplified structure and was used to perform the SA and NLRHA by using OpenSees for the parametric study. Fig. 3 shows the DM model with dual BRB-outrigger system. The BRBs are modeled by using truss elements, while the others are modeled using beam column elements. The material properties for the BRB elements are bilinear with a

post-yield stiffness ratio of 0.01, and the other members are linearly elastic. The length of each BRB is 1m. The perimeter column bases are free to rotate. The mass is distributed evenly on the height of core structure with a spacing of 1m.

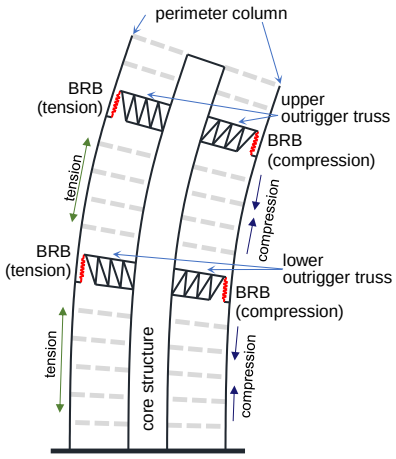

Fig. 1 – Deformed dual BRB-outrigger system

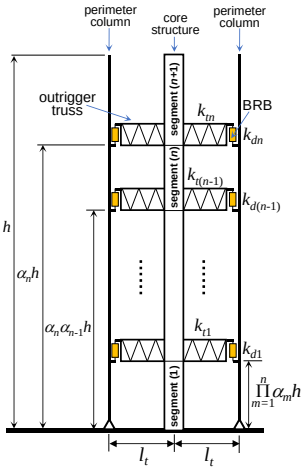

Fig. 2 – Simplified structure

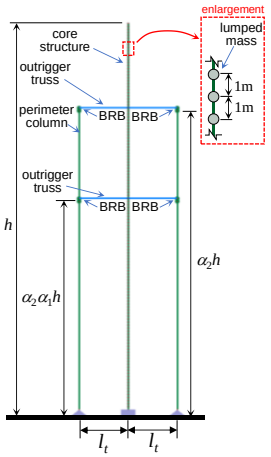

Fig. 3 – DM model

2.2 Parameter definitions

This study focuses on investigating the seismic performance of dual BRB-outrigger systems. Dimensionless parameters are introduced based on dual BRB-outrigger systems. The outrigger stiffness parameter S_{bc2} is defined as the ratio of rotational stiffness provided by the upper BRB-outrigger, when BRB axial stiffness is infinity, to the rotational stiffness of core structure as follows:

$$S_{bc2} = \left(\frac{l_t^2}{1/k_t + \alpha_2/k_c} \right) \Big/ \left(\frac{EI}{h} \right) = \frac{l_t^2 h}{EI\left(1/k_{t2} + \alpha_2/k_c\right)} = \frac{l_t^2 h k_c}{EI\left(R_{dt2}/R_{d2c} + \alpha_2\right)} \tag{2}$$

Where k_c and EI are the perimeter column axial stiffness with a length of h and the flexural rigidity of the core structure, respectively. R_{dt2} ($=k_{d2}/k_{t2}$) and R_{d2c} ($=k_{d2}/k_c$) are the BRB stiffness parameters. The value of S_{bc2} is used to indicate the magnitude of the outrigger effect on structure. The greater the value of S_{bc2}, the greater the outrigger effect. The outrigger effect can be enhanced by a longer outrigger truss span (l_t), stiffer outrigger trusses, and stiffer perimeter columns (greater k_t and k_c). In addition, for very tall buildings, the value of EI/h could significantly increase because of the higher seismic demand. Therefore, the outrigger truss member and perimeter column sizes should be increased in order to meet the desired outrigger stiffness parameter. The BRB parameter R_{d2c} ($=k_{d2}/k_c$) is defined as the ratio of the BRB axial stiffness in the upper outrigger (k_{d2}) to the perimeter column axial stiffness (k_c). In design practices, the perimeter column sizes are primarily designed according to the gravity load requirements. Therefore, R_{d2c} can provide engineers with a quick estimation of the required BRB sizes. The second BRB parameter R_{kd} ($=k_{d1}/k_{d2}$) is defined as the ratio of the axial stiffness of the BRB in the lower outrigger (k_{d1}) to the axial stiffness of the BRB in the upper outrigger (k_{d2}). When R_{kd} is greater than 1.0, the BRB in the lower outrigger is stiffer than the upper one, and vice versa. If R_{kd}=0, it is a single BRB-outrigger system. The parameter R_{dtj} is used to describe the ratio of k_{dj} to k_{tj} for the j^{th} level BRB-outrigger. In order to generate sufficient deformation demand on the BRBs, the R_{dtj} should be as small as possible. For simplicity, the values of R_{dt1} and R_{dt2} are set as 0.1 for the dual BRB-outrigger system in this study.

2.3 Spectral analysis

The SA procedure, incorporating an equivalent damping ratio [6] in order to consider the effect of inelastic deformation of BRBs, is used to evaluate the seismic performance of the dual BRB-outrigger system. The response of each mode is calculated separately and then combined by using the square root of the sum of the

squares (SRSS) rule. It is anticipated that the yielding of the BRB only results in a marginal decrease in the BRB-outrigger system stiffness. Therefore, it is assumed that the modal superposition principle based on elastic mode shapes remains applicable when the BRBs deform inelastically [7]. The maximum roof drift (θ_{max}), maximum inter-story drift (γ_{max}), core structure base shear ($V_{c,max}$), and overturning moment ($M_{c,max}$) are calculated based on the SRSS superposed deformed shape. As the BRBs in multiple BRB-outrigger systems would not yield simultaneously, this study uses the DM model to perform a modal pushover analysis (MPA) by using OpenSees to obtain the base shear and roof displacement relationship. Fig. 4a shows a MPA curve of the ith mode, where ytop,i is the roof displacement when the first BRB yields, K_i is elastic modal stiffness, and $K_{eq,i}$ is the equivalent stiffness when the roof displacement reaches its maximum value of $y_{max,i}$. It should be noted that the lateral force pattern used in the MPA remains the same as the elastic mode shape even after the BRB yields. The equivalent damping ratio ($h_{eq,i}$) of the ith mode response with a ductility of μ_i is calculated as follows:

$$h_{eq,i} = h_0 + \frac{1}{y_{\max,i}} \int_{y_{top,i}}^{y_{\max,i}} \frac{E_d(y)}{4\pi E_s(y)} dy, \quad \mu_i = \frac{y_{\max,i}}{y_{top,i}} \tag{3}$$

Where $E_d(y)$ and $E_s(y)$ are the energy dissipated by the BRB-outrigger system per loop and the strain energy with a roof displacement of y (Fig. 4b), respectively, and h_0 is the inherent damping ratio. The h_0 is assumed to be 0.02 for each mode in this study. The response spectrum is reduced because of the increased damping ratio by using the reduction factor $D_{h,i}$ expressed as follows [8]:

$$D_{h,i} = \sqrt{\frac{1+\kappa h_0}{1+\kappa h_{eq,i}}}, \quad \begin{matrix} \kappa = 25 \text{ for observed ground motions} \\ \kappa = 75 \text{ for artifical ground motions} \end{matrix} \tag{4}$$

The maximum roof displacement ($y'_{max,i}$) can be estimated as follows:

$$y'_{\max,i} = D_{h,i} S_d\left(T_{eq,i}, h_0\right) \Gamma_i \phi_i(h) \tag{5}$$

Where $T_{eq,i}$ is the equivalent vibration period, Γ_i is the i^{th} modal participation factor, and $\phi_i(h)$ is the roof displacement in the ith mode shape. $S_d(T, h_d)$ is the spectral displacement at period T and damping ratio h_d. In this study, the spectral displacement is calculated based on the design acceleration spectrum as shown in Fig. 5. After the first computation, replace the $y_{max,i}$ in Eq. 3 with $y'_{max,i}$ if they differ significantly. The calculation of the maximum roof displacement is an iterative procedure, and it should be continued until the $y_{max,i}$ used in computing $h_{eq,i}$ in Eq. 3 is sufficiently close to the $y'_{max,i}$ obtained from Eq. 5. In this study, the iteration is performed until the difference between $y_{max,i}$ and $y'_{max,i}$ become smaller than 5%. The response of the first four modes are calculated separately, and then combined using the SRSS method.

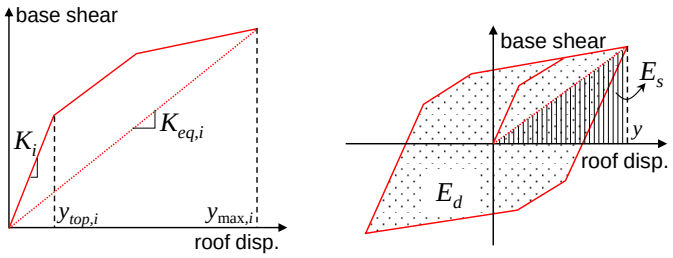

(a) (b)

Fig. 4 – Relationship (a) between base shear and roof displacement, and (b) between E_d and E_s

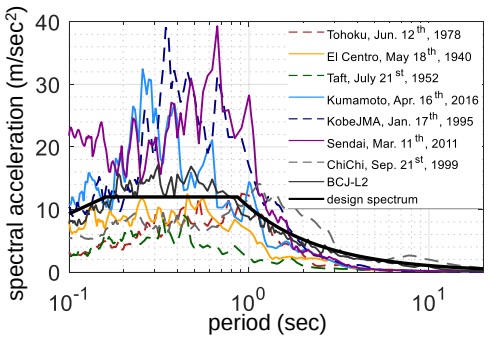

Fig. 5 – Response spectra of ground motions adopted in NLRHA

2.4 Nonlinear response history analysis

The NLRHA was performed using eight ground motions. Fig. 5 shows the spectra of the eight ground motions before scaling. For each of the analyses in NLRHA procedure, the spectral accelerations of the ground motions are scaled so that the mean of the spectral accelerations fit the design spectral acceleration within the range $0.2T_1$ to $1.5T_1$, where T_1 is the 1st mode period. A Rayleigh damping ratio of 0.02 for the 1st and 2nd modes was applied for all NLRHA. The means of the NLRHA results obtained from the eight ground motions are used to verify the SA results.

3. Analysis procedure of parametric study

Table 1 shows the analytical models used in this study. The 16-story, 32-story, 64-story, and 96-story models have heights of 64m, 128m, 256m, and 384m, respectively. The mass of each story is 900ton for all analytical models. The magnitude of the outrigger effect is indicated by S_{bc2} value when α_2 is 0.7. The outrigger effect is set smaller for taller building, because of the longer perimeter columns providing smaller values of k_c and greater values of EI because of higher seismic demand for taller buildings. The values of EI are selected so that the fundamental vibration period of the core structure is within a realistic range (for example $0.03h$). The value of R_{d2c} ranges from 0.1 to 3, and the value of R_{kd} is set as either 0 (single BRB-outrigger case), 0.5, 1, or 3. In each analysis set, with the selected R_{d2c} and R_{kd} values, the α_1 and α_2 vary from 0 to 1, and the value of k_c can be calculated by using Eq. 2. The value of R_{dt} is set as 0.1 in every analysis in the parametric study.

Table 1 – Parameters of analytical models

model	h (m)	l_t (m)	EI (kN-m^2)	S_{bc2} when α_2=0.7	fundamental period of core structure (sec)	R_{d2c}	R_{kd}
16-story	64	16	4.1×10^9	3.03	1.74	0.1, 0.5, 1, 1.5, 2, 2.5, 3	0, 0.5, 1, 3
16-storyB	64	14.5	4.1×10^9	2.48	1.74		
16-storyC	64	12.8	4.1×10^9	1.93	1.74		
32-story	128	16	1.6×10^{10}	1.38	3.50		
32-storyD	128	13.8	1.6×10^{10}	1.02	3.50		
64-story	256	16	6.5×10^{10}	0.66	6.92		
96-story	384	16	2.2×10^{11}	0.30	9.76		

The BRB yield deformation ($u_{d,y}$) is critical as it determines when the BRBs start yielding and dissipating energy. If $u_{d,y}$ is too large, the BRB could only slightly yield, or even remain elastic, during an earthquake, which would result in a low energy dissipation efficiency. However, if $u_{d,y}$ is too small, the BRB could easily yield even during a small earthquake, or fracture due to low-cycle fatigue before the end in a moderate earthquake. In this study, the BRB yield deformations are determined as follows. The first step is to calculate the spectral lateral deformed shapes of the first four modes of the structure based on the design spectrum. The second step is to combine the spectral deformed shapes of the first four modes using SRSS method. The combined deformed shape is then scaled until the roof drift reaches θ_r, which is the maximum allowable elastic roof drift limit, for example 1/750. The axial deformations of the BRBs under this combined deformed shape with the roof drift ratio of θ_r are adopted as the yield deformations. As the BRBs are deformation-dependent energy dissipation devices, it is believed that this combined deformed shape should best represent the deformed shape right before the two BRBs yield.

3. Analysis results

As the BRB-outriggers increase the system stiffness to reduce the seismic response by applying resisting moments on the core structure, the outriggers at the elevations that result in greatest drop of vibration period indicates that the outrigger effect is the greatest. It is anticipated that the optimal outrigger elevations in

minimizing seismic responses are also the outrigger elevations that have the greatest outrigger effect. Fig. 6 shows the 1st and 2nd mode vibration period distributions with respect to α_1 and α_2 for the 64-story model when R_{d2c} equals to 1 and 3 and R_{kd} equals to 1 and 3. The 1st mode vibration period distributions indicate that when α_2 is approximately 0.7 to 0.8, and when α_1 is approximately 0.6 to 0.7, the vibration periods are smallest. The 2nd mode vibration periods are the smallest when α_2 is around 0.8 to 0.9 and when α_1 is around 0.2 to 0.3. In addition, increasing R_{d2c} and R_{kd} stiffens the system, and causes the vibration period to decrease.

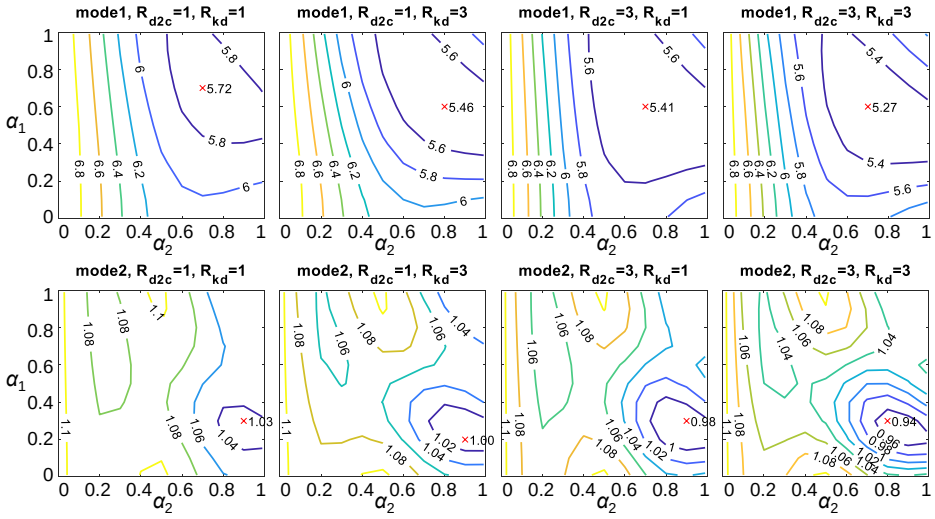

Fig. 6 – The 1st and 2nd mode vibration periods (sec) of 64-story model

Fig. 7 shows the yield deformations of BRB_1 ($u_{d,y1}$) and BRB_2 ($u_{d,y2}$) of a 64-story model with θ_r=1/750 when R_{d2c}=1 and 3 and R_{kd}=1 and 3. The $u_{d,y2}$ is maximum when α_2 is approximately 0.5 to 0.6 and α_1 is 0. The $u_{d,y1}$ is maximum when α_1 is approximately 0.5 and when α_2 is 1. As the lower BRB-outrigger is closer to the upper BRB-outrigger, $u_{d,y2}$ decreases and $u_{d,y1}$ increases. In addition, a stiffer BRB (greater R_{d2c} or R_{kd} values) results in a smaller $u_{d,y}$. The differences between $u_{d,y2}$ and $u_{d,y1}$ would be greater if R_{kd} is greater than 1 (when k_{d1} is greater than k_{d2}). The outrigger elevations that create the largest $u_{d,y2}$ or $u_{d,y1}$ could be also the optimal outrigger elevation, as they are in the most efficient configuration in generating the maximum deformation demand for the BRBs under the same θ_r. Based on the vibration period and yield deformation distributions, the optimal upper and lower outrigger elevations should be approximately 0.6 to 0.8 and 0.5 to 0.6, respectively.

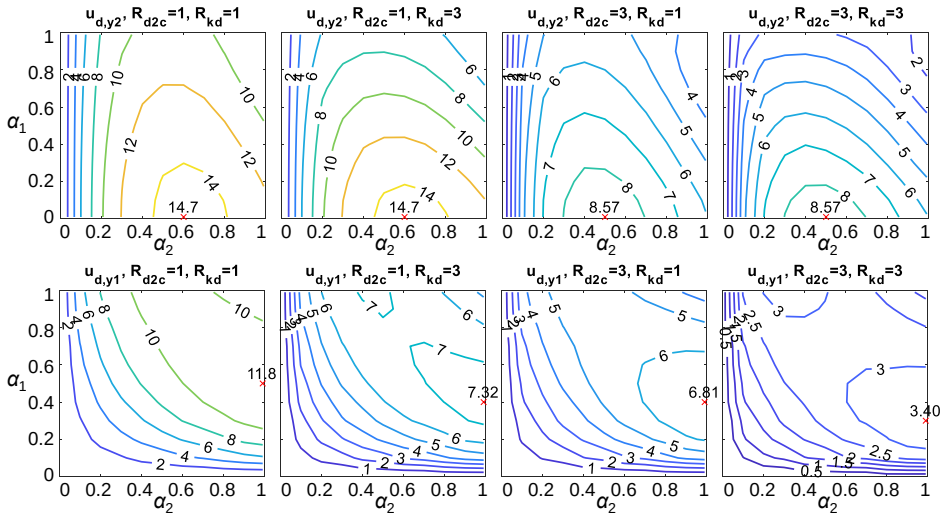

Fig. 7 – BRB yield deformations of 64-story model (unit: mm)

Figs. 8a and 8b show the analysis results of θ_{max}, γ_{max}, maximum perimeter column axial force ($C_{1,max}$), and maximum overturning moment at the core structure base ($M_{c,max}$) of the 16-story model when α_1 and α_2 vary from 0 to 1, R_{d2c} is 0.1, 1, and 3, and R_{kd} is 1 and 3. The results of the single BRB-outrigger cases can be identified from Fig. 8 when α_1 is 0. The SA well estimates the results of θ_{max} if compared with the NLRHA results. The trends of θ_{max}, γ_{max}, and $M_{c,max}$ with respect to the outrigger elevations are similar. The values of θ_{max}, γ_{max}, and $M_{c,max}$ primarily change with α_2, and the changes in α_1 only marginally affect the responses. It appears that the upper BRB-outrigger dominates the overall response, and the presence of the lower BRB-outrigger assists in further enhancing the performance. The values of θ_{max}, γ_{max}, and $M_{c,max}$ are minimum when α_2 and α_1 are approximately 0.7 and 0.6, respectively, and decrease with increasing R_{d2c}. This suggests that a greater value of R_{d2c} (stiffer BRB) provides a greater outrigger effect in mitigating the seismic response. However, as can be seen in Fig. 8, the decrease in seismic response when R_{d2c} increases from 0.1 to 1 is significantly greater than when R_{d2c} increases from 1 to 3. This suggests that the reduction in seismic response is not proportional to an increase in R_{d2c}. In addition, $C_{1,max}$ is maximum when α_2 is approximately 0.6, which is also the outrigger elevation that best reduces the seismic response. In addition, $C_{1,max}$ is almost doubled when R_{d2c} increases from 0.1 to 1 and from 1 to 3. The analysis results indicate that the benefit of reducing seismic responses by increasing R_{d2c} becomes negligible when R_{d2c} is too large, however, the $C_{1,max}$ keeps increasing at the same rate with increasing R_{d2c}. Too large value of $C_{1,max}$ is not desirable, as it increases the perimeter column sizes. If Fig. 8a is compared with 8b, the seismic response reductions are slightly increased when the value of R_{kd} changes from 1 to 3. As the upper BRB-outrigger dominates the overall response, the changes in α_2 and R_{d2c} would affect the overall response more than the changes in α_1 and R_{kd}.

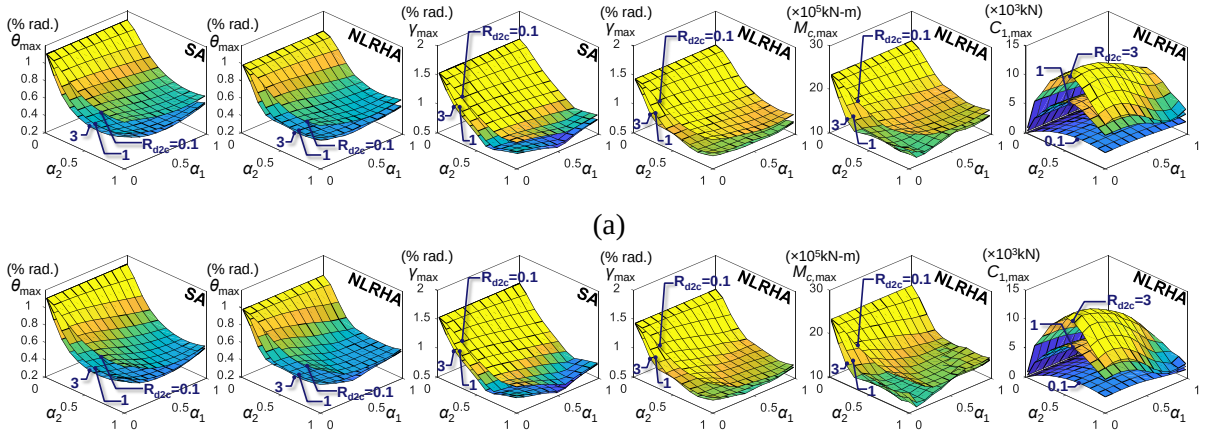

(a)

(b)

Fig. 8 – SA and NLRHA results for 16-story model with (a) R_{kd}=1 and (b) R_{kd}=3

Figs. 9 to 12 show the reductions in θ_{max}, γ_{max}, and $M_{c,max}$ (reduction factor, in percentage) when compared with the structure without outriggers, and the values of $C_{1,max}$ for each analytical model when R_{d2c}=1 and 3 and R_{kd}=1. The shapes of the reduction factor distribution of θ_{max}, γ_{max}, and $M_{c,max}$ are similar. The reduction factors primarily change with α_2, and the values are minimum (greatest reduction) when α_2 is between 0.7 and 0.8. The effect of varying α_1 is negligible when α_2 is smaller than 0.4. Even when α_2 is at its approximate optimal elevation (between 0.7 and 0.8), the changes in the reduction factor because of varying α_1 is limited to within 10%. This suggests that, when α_2 is smaller than 0.4, the presence of the lower outrigger has no contribution in achieving better seismic performance. In addition, when α_2 is at its optimal elevation and α_1 is approximately 0.4 to 0.7, θ_{max} and γ_{max} can be best reduced. The trends of θ_{max} and γ_{max} distributions with respect to α_2 and α_1 are similar to the 1st mode period trend as shown in Fig. 6. This suggests that the outrigger elevations that have the greatest outrigger effect on the system is also the optimal elevation in order to achieve minimum θ_{max} and γ_{max}. The $C_{1,max}$ results indicate that the perimeter column axial force is maximum when α_2 is approximately 0.5 to 0.7, which is also the optimal elevation of α_2 that best reduces the θ_{max}, γ_{max}, and $M_{c,max}$ responses. In the models with the same number of stories, the increase in R_{d2c} from 1 to

3 (increase both the axial stiffness of BRB_1 and BRB_2 by 3 times) only increases the overall reduction by approximately 5%, however, the perimeter column force demand ($C_{1,\max}$) is increased by 50%. Based on the analysis results, a greater value of S_{bc2} suggests a greater outrigger effect that, therefore, results in smaller reduced seismic response. In summary, the optimal upper outrigger elevations (α_2) are approximately 0.7 and 0.8. For the lower outrigger elevation (α_1), the optimal α_1 is in the range of 0.4 to 0.7 if the first priority is to mitigate $\theta_{\max}$ and $\gamma_{\max}$, and the optimal α_1 is in the range of 0.2 to 0.4, if mitigating $M_{c,\max}$ is critical. In order to increase the seismic response reductions, increasing the value of S_{bc2} when α_2=0.7 would be more efficient than increasing the value of R_{d2c}.

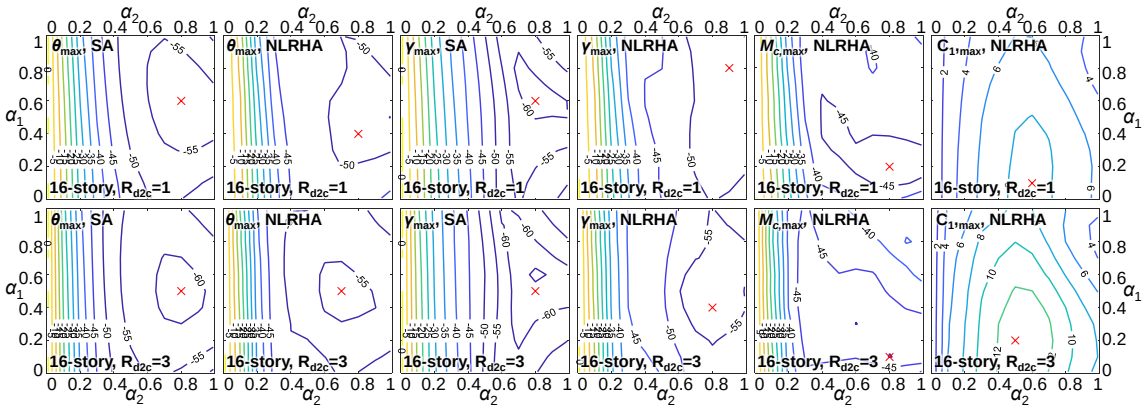

Fig. 9 – Reduction factor distributions of 16-story model when R_{kd}=1

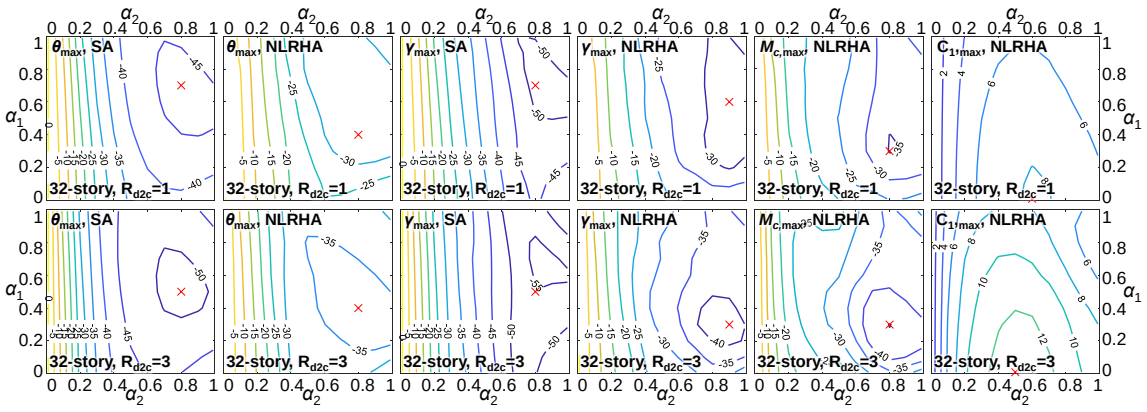

Fig. 10 – Reduction factor distributions of 32-story model when R_{kd}=1

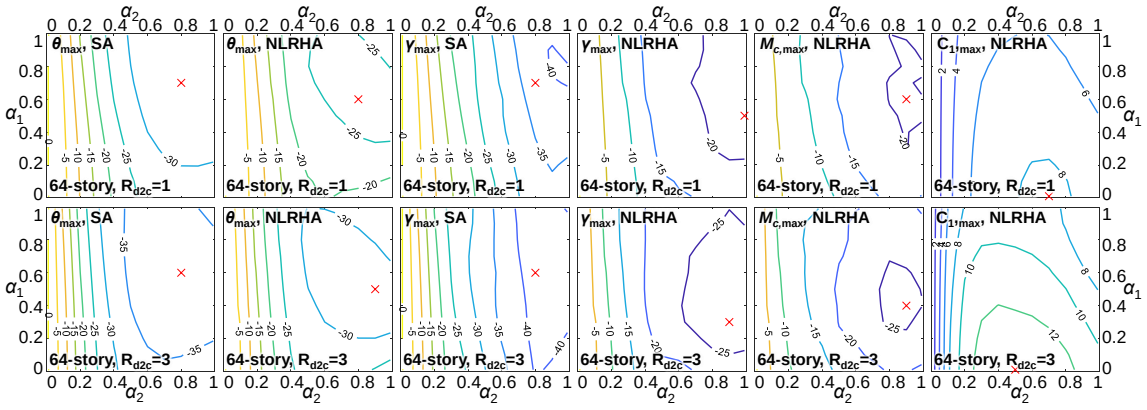

Fig. 11 – Reduction factor distributions of 64-story model when R_{kd}=1

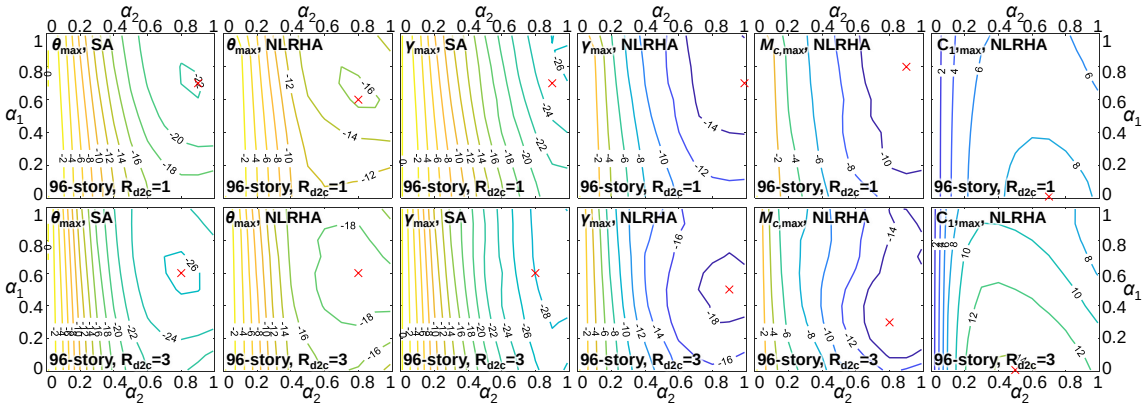

Fig. 12 – Reduction factor distributions of 96-story model when R_{kd}=1

Figs. 13 to 15 show the reductions (in percentage) in θ_{max}, γ_{max}, and $M_{c,max}$ with respect to R_{d2c}, S_{bc2}, and R_{kd} for the cases when α_2 is 0.5, 0.7, and 0.9 and when α_1 is 0.3 and 0.6. It should be noted that the θ_{max} and γ_{max} reduction factor distributions shown in Figs. 13 to 15 are based on the SA results, and the $M_{c,max}$ reduction factor distributions are based on the NLRHA results. The shapes of the reduction factor distributions of θ_{max}, γ_{max}, and $M_{c,max}$ are similar. The greater values of R_{d2c} and S_{bc2} suggest a greater outrigger effect indicating a smaller seismic response. However, the rate of increase in the reduction becomes slower, or even stops, as R_{d2c} increases under a fixed value of S_{bc2}. Therefore, the optimal value of R_{d2c} should be approximately 0.5 to 1.5. When the value of R_{d2c} is greater than 1.5, the required BRB axial stiffness increases (increasing the cost of the BRB), however, the reduction in seismic responses becomes less efficient. In addition, if the cases when α_2 varies between 0.5 (Fig. 13), 0.7 (Fig. 14), and 0.9 (Fig. 15) are compared, when α_2 is changed from 0.5 to 0.7, the reductions in θ_{max} and γ_{max} increase by approximately 10%, and when α_2 is changed from 0.7 to 0.9, the reductions in θ_{max} and γ_{max} increase by approximately 3%, and the changes in the $M_{c,max}$ reductions are insignificant. However, when α_1 decreases from 0.6 to 0.3, the $M_{c,max}$ reductions increase by approximately 5% for the cases when α_2 is 0.5 (Fig. 13), and increase by approximately 10% for the cases when α_2 is 0.7 (Fig. 14) and 0.9 (Fig. 15). The analysis results suggest that the optimal upper BRB-outrigger elevation in order to mitigate θ_{max} and γ_{max} is approximately 0.7 to 0.9. In addition, if α_2 is within its optimal range, the reduction in $M_{c,max}$ is optimal when the lower BRB-outrigger is close to the core structure base. When R_{kd} changes from 1 to 3, the θ_{max} and γ_{max} reductions increase by approximately 3% and 5% when α_1 is 0.3 and 0.6, respectively, and the increases in the $M_{c,max}$ reductions are approximately 5% and 3% when α_1 is 0.3 and 0.6, respectively. Therefore, it appears that the method of increasing R_{kd} is efficient to reduce θ_{max} and γ_{max} when α_1 is approximately 0.6, and to reduce $M_{c,max}$ when α_1 is approximately 0.3.

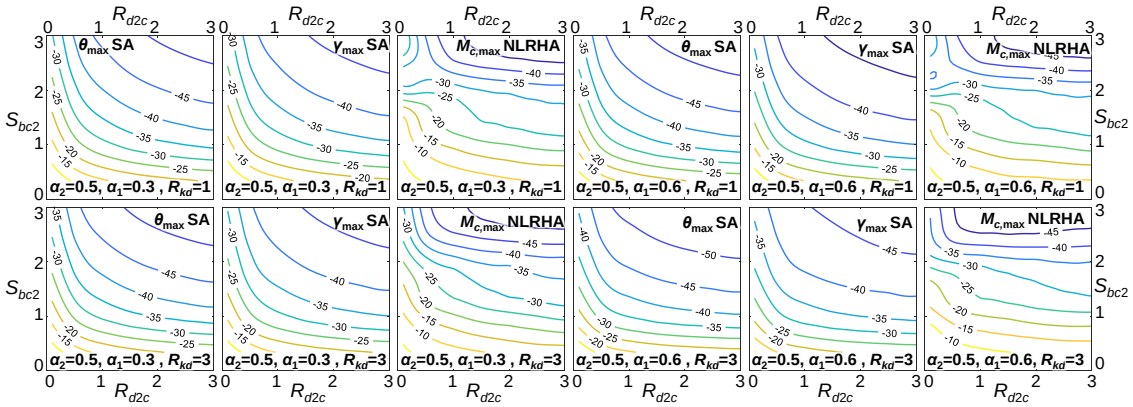

Fig. 13 – Reduction factors distribution with respect to R_{d2c} and S_{bc2} when α_2 is 0.5

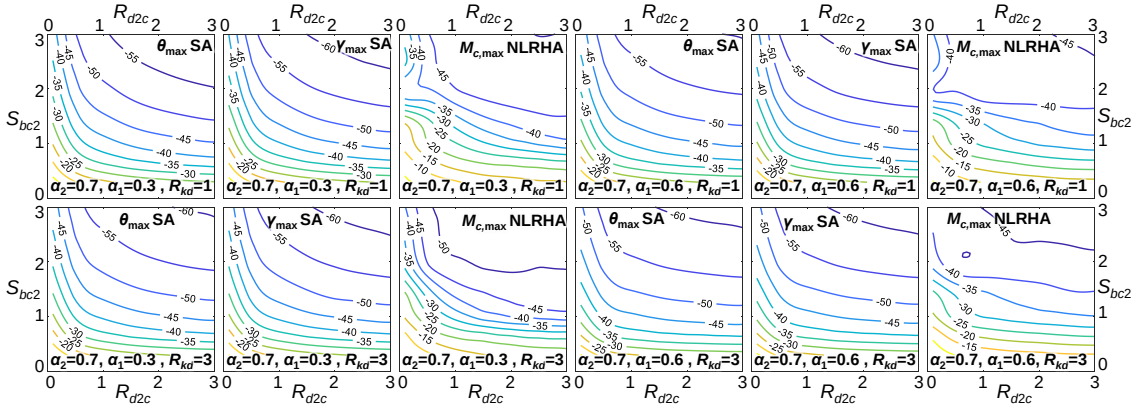

Fig. 14 – Reduction factors distribution with respect to R_{d2c} and S_{bc2} when α_2 is 0.7

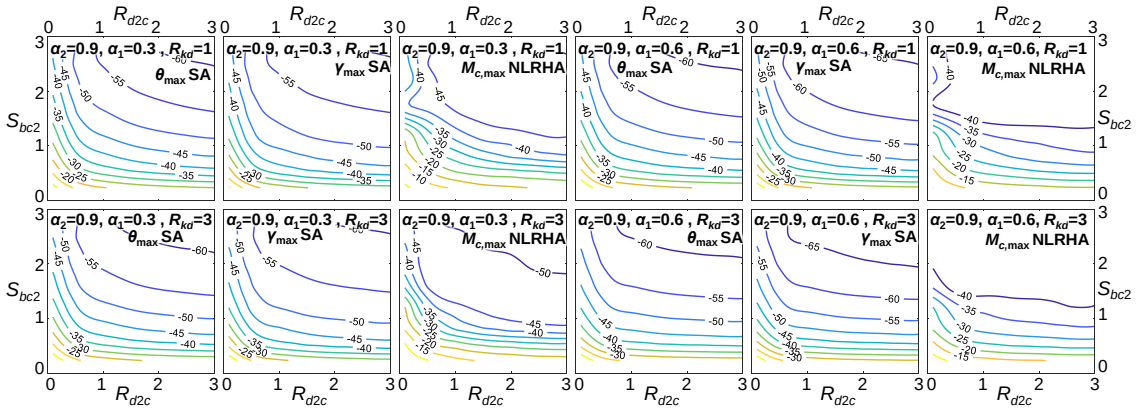

Fig. 15 – Reduction factors distribution with respect to R_{d2c} and S_{bc2} when α_2 is 0.9

Based on the analysis results, the optimal upper (α_2) and lower (α_1) BRB-outrigger elevations so as to minimize the seismic response are approximately 0.7 to 0.8 and 0.4 to 0.7, respectively. For design practices, selecting the appropriate outrigger elevations should be the first priority as they have the greatest effect on the overall seismic performance. S_{bc2} should be selected as large as possible as it determines the magnitude of the outrigger effect. The value of R_{d2c} should be limited between 0.5 and 1.5, as too large R_{d2c} value increases the cost of the BRB and the additional seismic reduction is insignificant. The lower BRB-outrigger further improves the seismic performance, and its optimal elevation depends on the design strategy. Placing the lower BRB-outrigger at the elevation where inter-story drift is too large could greatly mitigate the inter-story response. Furthermore, placing the lower BRB-outrigger at α_1 approximately 0.4 to 0.7 could best reduce θ_{max} and γ_{max}. If the core structure base overturning moment is critical, the lower BRB-outrigger can be placed at an α_1 of approximately 0.2 to 0.4. The value of R_{kd} is recommended as 1.0, and it could be used to fine-tune the design as changing it from 1 to 3 only affects the seismic response within 5% to 10% based on the analysis results.

4. Conclusions

(1) The SA procedure using the equivalent damping ratio to evaluate the hysteretic responses of the BRBs. The responses from the first four modes were considered in the SA. The results obtained from SA and NLRHA exhibited similar trends.

(2) For the dual BRB-outrigger systems, the parameters θ_{max}, γ_{max}, and $M_{c,max}$ primarily changed with the upper BRB-outrigger elevation (α_2). The upper BRB-outrigger dominates the seismic response, and the presence of additional lower BRB-outrigger further improved the seismic response by reducing θ_{max}, γ_{max}, and $M_{c,max}$.

(3) By utilizing the BRB-outrigger system, the optimal α_2 and α_1 in order to minimize θ_{max} and γ_{max} were 0.7 to 0.8 and 0.4 to 0.7, respectively. The value of $M_{c,max}$ could be best reduced when α_1 was between 0.2 and 0.4. In addition, the lower BRB-outrigger could be placed at the elevation where the inter-story drift ratio was too large to mitigate the excessive inter-story drift response. The optimal α_1 and α_2 were not significantly affected by the values of S_{bc2}, R_{d2c}, and R_{kd}. However, $C_{1,max}$ may increase most when α_2 was between 0.5 and 0.7.

(4) Increasing R_{d2c} could reduce θ_{max}, γ_{max}, and $M_{c,max}$, but the rate of reduction decreased, or even stopped, with increasing R_{d2c}. The optimal R_{d2c} should be approximately 0.5 to 1.5.

5. References

[1] Smith R, Willford M (2007): The damped outrigger concept for tall buildings. *The structural design of tall and special buildings*, **16** (4), 501-517.

[2] Huang B, Takeuchi T (2017): Dynamic response evaluation of damped-outrigger system with various heights. *Earthquake spectra*, **33** (2), 665-685.

[3] Chen Y, McFarland D, Wang Z, Spencer B, Bergman L (2010): Analysis of tall building with damped outriggers. *Journal of structural engineering*, **136** (11), 1435-1443.

[4] Lin PC, Takeuchi T, Matsui R (2018): Seismic performance evaluation of single damped-outrigger system incorporating buckling-restrained braces. *Earthquake Engineering and Structural Dynamics*, **47** (12), 2343-2365.

[5] Lin PC, Takeuchi T, Matsui R (2019): Optimal design of multiple damped-outrigger system incorporating buckling-restrained braces. *Engineering Structures*, **194**, 441-457.

[6] Newmark M, Rosenblueth E (1971): *Fundamentals of earthquake engineering*, Prentice-Hall, Inc., Englewood Cliffs, N.J., USA.

[7] Chopra A, Goel R (2002): A modal pushover analysis procedure for estimating seismic demands for buildings. *Earthquake Engineering and Structural Dynamics*, **31** (3), 561-582.

[8] Kasai K, Fu Y, Watanabe A (1998): Passive control system for seismic damage mitigation. *Journal of Structural Engineering*, **124** (5), 501-512.

